EVOLVING IMPACTS OF CHRONIC COASTAL HAZARDS UNDER A CHANGING CLIMATE IN CASCADIA, USA

MEREDITH LEUNG¹, LAURA CAGIGAL², FERNANDO MENDEZ²,
PETER RUGGIERO¹

- College of Earth, Ocean, and Atmospheric Science, Oregon State University, 104 CEOAS Administration Building, Corvallis, OR 97331, USA. leungmer@oregonstate.edu, pruggiero@coas.oregonstate.edu.
- Dep. de Ciencias y Técnicas del Agua y del Medio Ambiente, Univ. de Cantabria, Spain. Av. De los Castros, s/n, 39005 Santander, Cantabria, Spain. <u>laura.cagigal@unican.es, fernando.mendez@unican.es</u>.

Abstract: Regional scale assessments of future chronic coastal hazard impacts are critical tools for adaptation planning under a changing climate. Probabilistic simulations of hazard impacts can improve these assessments by explicitly attempting to quantify uncertainty and by better simulating dependence between complex multivariate drivers of hazards. In this study, probabilistic future timeseries of total water levels (TWLs) are generated from a stochastic climate emulator (TESLA; Anderson et al., 2019) for the Cascadia region, USA for use in a chronic hazard impact assessment. This assessment focuses on three hazard metrics: collision, overtopping and beach safety, and also introduces a novel hotspot indicator to identify areas that may experience dramatic changes in hazard impacts compared to present day conditions. Results are presented for a subset of the Cascadia region (Rockaway Beach Littoral Cell, Oregon) to demonstrate the power of the probabilistic impact assessment approach. The results highlight how useful spatially varying, scenario-based hazard impacts assessments and hotspot indicators are for identifying which areas and types of hazards may require increased adaptation support. This approach enables us to piece apart the relative uncertainty of hazards as driven by SLR versus natural variability (caused by variation in climate, weather, and hydrodynamic drivers).

Introduction

Hazardous coastal flooding and erosion events are becoming more frequent and intense due to a changing climate and evolving societal pressures. Rising sea levels and shifting storminess patterns (e.g., Sweet et al., 2022; Erikson et al., 2022), combined with increasing financial and cultural investment in coastal regions (Lincke et al., 2022), compound hazard stressors in coastal communities. To alleviate the economic and social costs of chronic flooding and erosion hazards, coastal communities need to take proactive steps toward relieving hazard stressors driven by both natural and human systems based on a comprehensive understanding of possible future risk (Haasnoot et al., 2019). Regional scale assessments of potential future hazard impacts are critical tools for enabling this comprehensive understanding, as they generate results on spatial and temporal

scales typically embedded in policy decision structures (Hibbard and Janetos, 2013).

Impact assessments of potential future chronic coastal hazards commonly adopt extreme value analysis (EVA) approaches (e.g., Vitousek et al., 2017, Taherkhani et al., 2020). EVA uses statistical techniques to characterize the intensity and frequency of previously unseen hazardous events based on the probability of extremes in the historical record. These techniques are powerful, generalizable, and well suited to practical applications (e.g., engineering or insurance) as they quantify hazards in terms of traditional engineering design criteria (i.e., extreme event return periods). However, EVA approaches can be less suited to analyses that wish to explore both chronic and extreme conditions together, or how the timing of events influences hazard impacts, as traditional EVA techniques explore the impacts of extremes in isolation. Furthermore, EVA can have challenges accurately quantifying extremes for hazards with complex multivariate drivers, as the dependence between drivers can be difficult to represent (Hamdi et al., 2021).

Probabilistic simulation modeling (e.g., Callaghan et al., 2008, Serafin and Ruggiero, 2014) is an alternative approach to assessing future hazards that can avoid some of the typical drawbacks of EVA described above (Toimil et al., 2020). Probabilistic methods simulate a range of potential outcomes, representing both chronic and extreme conditions by varying the timing and intensity of environmental variables driving hazards. This enables exploration of how the timing of events can shape hazard impacts and can help dissect which environmental variables ultimately drive hazardous conditions (e.g., Toimil et al., 2021). When combined with climate aware approaches that incorporate the uncertainty associated with forecasted carbon emission scenarios, regional sea level rise (SLR) rates, decadal to intra-decadal oscillations in climate variability, etc., probabilistic approaches become a powerful tool for assessing and constraining the uncertainty of future hazard impacts (Kopp et al., 2019).

This paper employs a stochastic climate emulator, TESLA (<u>Time varying Emulator for Short and Long-term Analysis of coastal flooding and erosion;</u> Anderson et al., 2019), to generate probabilistic future total water levels (TWLs) for a regional scale impact analysis in Cascadia, USA. TESLA combines machine learning approaches and statistical models to generate hypothetical chronologies of the full suite of TWL drivers. TESLA also links climate and weather to the multivariate drivers of hazardous events, enabling the exploration of dependence structures between hazards, hydrodynamic variables, and associated climate and weather conditions.

In this study, TWL generation and impact analysis is performed for the outer coastline of Cascadia, USA, ranging from Northern California to Northern

Washington. Many Cascadia coastal communities have already begun to feel the effects of climate change through increased nuisance flooding events and erosion rates (Light, 2021; Sweet et al., 2022; Taherkhani et al., 2023). While hazards are expected to continue to intensify under projected SLR and changing patterns of storminess (Shope et al., 2022), the range of potential hazard conditions (timing, frequency, magnitude, and location) that communities should prepare for are highly uncertain. To begin to constrain that uncertainty, here we assess three hazard metrics: collision, overtopping, and beach safety. These metrics are calculated for four different SLR scenarios, with 100 probabilistic simulations of hourly TWL drivers for 2020-2100, and at 100m resolution across the entire Cascadia coastline. We also identify 'hotspots' of hazard impacts – areas that will see a dramatic change between present day hazard conditions and future conditions, to highlight areas which may benefit from greater investment in adaptation resources.

Study Site: Cascadia, USA

The wave climate of the Cascadia region is notable for its severity. Winter storms frequently produce long period waves with heights exceeding several meters (Allan et al., 2015). Previous TWL studies conducted on the US West Coast have highlighted that wave driven runup accounts for the largest fractional contribution to extreme TWL events (>50%) and that the most extreme events occur when large astronomical tide and high wave events coincide (Serafin et al., 2017). In addition, local bathymetry and beach morphology are dominant controls in determining onshore impacts of extreme TWLs, as they can cause large nonlinear changes to the number of hazard impact hours with only small variations in TWL (Serafin et al., 2019).

El Niño Southern Oscillation (ENSO) events have also been shown to contribute to hotspot erosion and increased flood risk in the Pacific Northwest (PNW) due to more extreme winter waves (~30% higher) and higher water levels (~0.2-0.3m) (Barnard et al., 2015; Barnard et al., 2017; Komar et al., 2011; Shope et al., 2022). Changes to ENSO event frequency and wave climate intensity are expected under climate change (Cai et al., 2015; Erikson et al., 2022). However, how these phenomena will evolve is not certain (e.g., Yu et al., 2017; Cai et al., 2018). As such, incorporating sources of climatic and weather driven uncertainty into water level projections is valuable for coastal communities and their planning efforts.

While impact analysis has been performed for the entire Cascadia coastline, this paper will present results for a subset of the region, the Rockaway Beach littoral cell in Tillamook County, Oregon (Figure 1), for the sake of simplicity and to demonstrate the capabilities of the methodology.

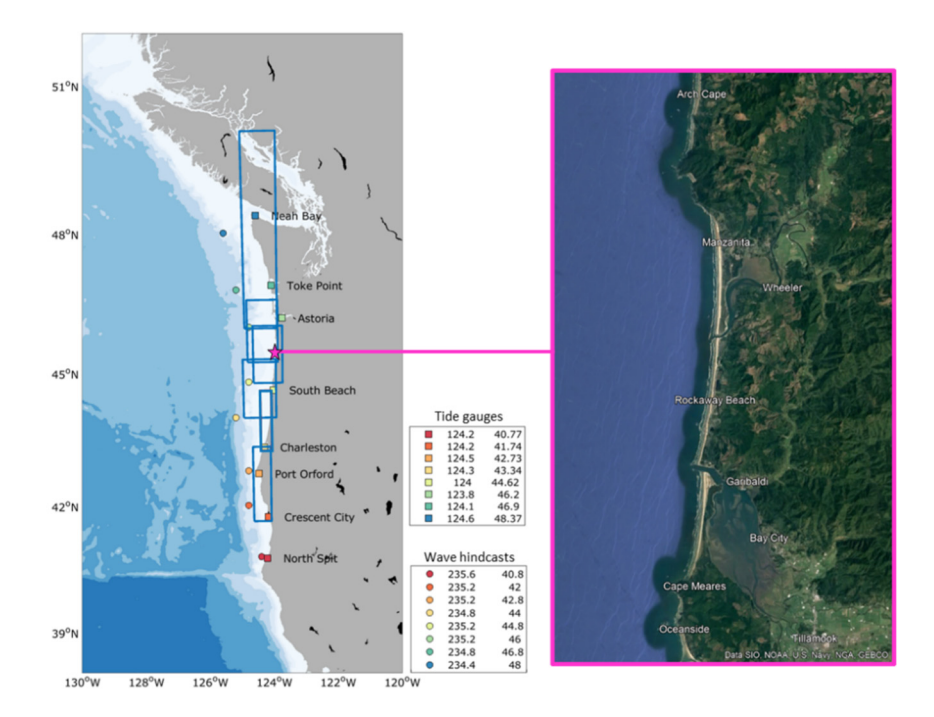


Figure 1. Location of TESLA hydrodynamic variable inputs (CAWCR wave hindcasts and NOAA tide gauges), hybrid nearshore wave transformation domains (SWAN Lookup Tables), and the subset region for which results will be presented.

Probabilistic Total Water Level Simulations

Total water levels represent the maximum elevation that water reaches on the coast. They are driven by atmospheric, oceanographic, and geomorphic processes and can be represented by the following equation:

$$TWL = SWL + R_{2\%} \tag{1}$$

Where $R_{2\%}$ represents the wave driven runup (2% exceedance level, e.g., Holman, 1986) and SWL represents the still water level. SWL can be further decomposed as the sum of several processes:

$$SWL = \eta_{MSL} + \eta_{AT} + \eta_{SE} + \eta_{SS} + \eta_{MMSLA}$$
 (2)

 η_{MSL} is the mean sea level, η_{AT} is the astronomical tide, η_{SE} is the seasonal signal, η_{SS} describes the atmospheric driven storm surge, and η_{MMSLA} represents interannual variability captured through monthly mean sea level anomalies.

We generate 100 simulations of hourly future TWLs at 100m resolution for the Cascadia region in two phases: first, through the simulation of offshore boundary conditions at eight semi-coupled TESLA nodes; second, through transformation of wave conditions and runup calculations using hybrid nearshore models and empirical runup formulas (Figure 2). TWLs are then combined with four probabilistic regional scale SLR scenarios associated with 0.5m, 1.0m, 1.5m, and 2.0m of global mean SLR by 2100 (Sweet et al., 2022).

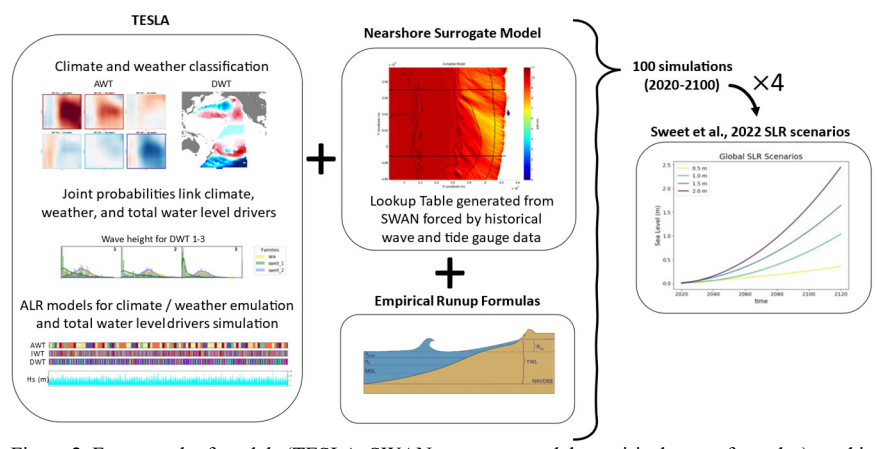


Figure 2. Framework of models (TESLA, SWAN surrogate model, empirical runup formulas) used in total water level simulation for the Cascadia region. 100 simulations are applied to four regionally scaled global sea level rise scenarios.

Probabilistic Simulation of Offshore Total Water Level Drivers: TESLA

The TESLA framework produces the offshore drivers of TWLs using a weather type-based approach, in which annual weather types (AWTs), intra-seasonal weather types (IWTs), and daily weather types (DWTs) are defined based on observed atmospheric and oceanographic variables. The weather types are then linked to hydrodynamic variables (e.g., wind waves, swell, storm surge) via joint probabilities, enabling simulation of new timeseries of these variables based on the probabilities of historical observations. A brief summary of the TESLA methodology (see Anderson et al., 2019 for more detail) is presented below:

The three weather types are generated using statistical techniques including principal component analysis and k-means clustering. Each weather type represents a different scale of climate and weather; AWTs depict large scale climate via ENSO patterns, IWTs represent the Madden Julien Oscillation (MJO), and DWTs depict synoptic weather patterns. New chronologies of the weather types are generated using autoregressive logistic regression models that are able

to reproduce the persistence, transition, and probability of occurrence of the weather types based on historical observations and model covariates (Antolinez et al., 2015).

TESLA simulates the persistence of waves during individual storm events using wave hydrographs. When consecutive days of the same DWT occur, they are grouped together as a single weather event. Each weather event is assigned a hydrograph that represents the ramp up to and ramp down from the maximum potential flooding within the weather system based on random sampling of parameterized historical hydrographs during the specified DWT. Wave and water level variables are sampled for each hydrograph using gaussian copulas, which are fit using the joint probabilities between the hydrodynamic variables and the weather type. Employing gaussian copulas maintains the historical dependence structures between sea state parameters and weather types while allowing for extrapolation from historical observations (Cagigal et al., 2020). While wave height evolves hourly based on hydrograph ramp up and down, other variables remain static for the duration of the hydrograph for simplicity. Monthly mean sea level is the only predictand not simulated through the hydrographs. Instead, it is simulated using a linear regression, for which three PCs derived from the AWTs and three PCs describing regional monthly-averaged synoptic weather serve as the inputs.

Following the methodology in Anderson et al., (2019), we constructed eight semi-coupled TESLA nodes along the Cascadia coastline at 1 degree latitude spacing. Here, semi-coupled indicates that the weather types are shared across all eight sites, while the hydrodynamic inputs, comprised of wave hindcasts from the Center for Australian Weather and Climate Research (CAWCR; Durrant et al., 2014; Smith et al., 2020) and tide gauges (NOAA, tidesandcurrents.noaa.gov), are unique to each location (Figure 1). As such, for a given TESLA simulation, large scale climate, intra-seasonality, and daily weather are consistent across the Cascadia region, but the offshore hydrodynamic variables are generated from local wave and water level observations.

Hybrid Nearshore Wave Transformation and TWL Calculation

To calculate wave driven runup components of TWLs, we use a combination of previously developed surrogate models for nearshore wave transformation (Allan et al., 2015) and empirical runup formulas. The surrogate models are comprised of interpolated lookup tables generated based on stationary SWAN modeling of historical water level and wave conditions. Offshore wave simulations from TESLA are input into the SWAN lookup tables and extracted at approximately the 20m contour line at 1km resolution. They are then back propagated to compute

alongshore varying deep-water wave conditions. While the surrogate models are capable of extracting waves every 100m in the alongshore direction, sensitivity testing revealed down-sampling to 1km significantly reduced computational expense with low impact to final TWL values.

Using the alongshore varying wave conditions (1km resolution) and lidar-derived geomorphology (100m resolution; Shope et al., 2021) as input into the Stockdon et al. (2006) empirical runup formula, we incorporate the wave driven component of TWLs into the simulated impact analysis for the Cascadia region.

The time evolving TESLA outputs are transformed over reference bathymetry and topography that does not change over time. Nearshore bathymetric data used in the SWAN models was derived from 1/3 arc-second (~10 m) DEMs downloaded from the NOAA's National Geophysical Data Center and onshore geomorphic data is derived from a US West Coast lidar dataset (Shope et al., 2021). Keeping bathymetry and topography static in this analysis is a necessary choice for impact studies of this scope (100 simulations, 80 years, regional scale), as existing models used for morphological evolution (e.g., XBeach, Delft3D) are largely designed for event-based simulations along a single beach (Roelvink et al., 2009). To evolve bathymetry and topography over the spatial and temporal scale of this study with available tools would therefore be inappropriate and would yield results with compounding errors. It is important to note, however, that since morphology is held static, the future TWLs and hazard impact projections presented here should not be interpreted as accurate forecasts, but rather as practical comparisons to present day conditions.

Coastal Hazard Impact Metrics

We assess coastal hazard impacts using three simple proxies (collision hours, overtopping hours, and unsafe beach hours) developed from well-established coastal hazard frameworks (Sallenger, 2000) and feedback from regional stakeholders (Table 1).

Collision and overtopping are classic proxies for dune face erosion or dune flattening and backshore flooding, respectively (Sallenger, 2000). Here we apply these metrics to dune-backed beaches in Cascadia, as well as areas with other backshore features (e.g., cliff-backed, armored, cobble beaches, etc.). While the erosional response to collision and overtopping for sandy and non-sandy backshore morphologies is different, the metrics can still indicate whether conditions that commonly lead to erosion or flooding are present.

Table 1. Description of Chronic Hazard Proxies

Collision Hours		Proxy for erosion backshore feature toe < TWL < backshore feature crest	
Overtopping Hours	Account.	Proxy for flooding TWL > backshore feature crest	
Unsafe Beach Recreation Hours		Proxy for usability of the beach (too narrow to play, work, etc.) Beach width < 10m during daylight hours	

The unsafe beach hours metric was developed through extensive engagement with stakeholders in the Cascadia region. Stakeholders highlighted that solely assessing flooding and erosion proxies tends to center hazard impact discussions on coastal property owners only. Stakeholders expressed interest in a proxy that can communicate how the general population may also be impacted by chronic coastal hazards. On their suggestion, we created a beach safety proxy that underscores how visitors to beaches (either for work or leisure) may feel unable to utilize the beach for their preferred activities based on its time-dependent width. To quantify beach safety, we track the number of daylight hours during which the beach is 'unsafe', or too narrow to comfortably recreate without safety concerns. The definition of 'too narrow' should be determined based on the unique conditions of a particular beach and how visitors use it. In the Rockaway Beach Littoral Cell presented here, a width of 10m was chosen through stakeholder input.

We track the evolution of impact metrics through the changes in the *percent impact hours*. This measurement sums the total hours in which conditions for hazard impacts are met during a particular time period and divides it by the total hours in that period. Here, we largely present the percent impact hours over the duration of decades to explore the influence of SLR on hazard impacts, but different durations can be chosen based on research focus or stakeholder needs.

Hotspot Identification

To identify areas that experience a large change in hazard impacts compared to present day conditions, we propose a novel normalized hotspot indicator:

$$Hotspot\ Indicator = Impact\ Multiplier \times Total\ Diff\ in\ Hours$$
 (3)

Where the *impact multiplier* is the factor by which the hazard impact increases from the initial to the final timestep, and the *total difference in hours* is the difference in impact hours between the final time step and the initial.

Results and Discussion

The Rockaway Beach Littoral Cell, hereafter called RBLC, currently experiences relatively low rates of collision (8.4% collision hours when averaged over space and 100 simulations), slightly higher rates of unsafe beach conditions (15.3%), and virtually no overtopping (0.12%). The 5th and 95th percentile uncertainty range bound these metrics by just a few percent for collision and beach safety hazards, and by less than 1% for overtopping. Table 2 shows a comparison of impact hours for RBLC associated with present-day conditions (0.0m SLR) and the impact hours of four different SLR scenarios by the end of the century.

Hazard Metric	Range	0.0m SLR	0.5m SLR	1.0m SLR	1.5m SLR	2.0m SLR
Collision	5 th pct	6.82 %	8.15 %	10.7 %	14.5 %	20.9 %
	Mean	8.40 %	9.99 %	12.9 %	17.3 %	24.3 %
	95 th pct	10.1 %	11.9 %	15.3 %	20.2 %	27.9 %
Beach Safety	5 th pct	12.1 %	14.2 %	18.1 %	23.8 %	32.4 %
	Mean	15.3 %	17.5 %	21.8 %	27.8 %	36.5 %
	95 th pct	18.8 %	21.2 %	25.7 %	31.9 %	40.7 %
Overtopping	5 th pct	0.06 %	0.09 %	0.14 %	0.24 %	0.39 %
	Mean	0.12 %	0.16 %	0.23 %	0.36 %	0.59 %
	95 th pct	0.18 %	0.23 %	0.33 %	0.51 %	0.80 %

Table 2. Spatially Averaged Rockaway Beach Impact Hours from 2090-2100

There are a few important results that we can gather from this table. First, under the different SLR scenarios, collision will increase to a range between 10% to 25% impact hours, unsafe beach hours increase to a range of 17.5% to 36.5%, and overtopping will remain close to zero with a range of 0.2% to 0.6% impact hours. As such the RBLC community may decide to focus adaptation efforts on erosion and beach safety hazards, as flooding will remain rare even under the most extreme SLR scenario. Second, as we go to higher SLR scenarios the uncertainty of hazard impacts increases along with the total number of impact hours. And

finally, the range of uncertainty associated with SLR exceeds the uncertainty associated with natural climate variability (derived from the 100 TESLA simulations) by the end of the century, but not greatly. For example, focusing on collision, the uncertainty range associated with SLR is 14.4%, but the uncertainty associated with natural climate variability goes up to 7%, indicating that the inherent variability of TWL drivers has a significant influence on the total uncertainty of hazard impacts and should not be ignored.

While averaging spatially over the littoral cell is a useful summary tool, it omits nuance associated with local bathymetry and topography. To explore the spatial variability of impact hazards in greater detail, hazard maps (e.g., Figure 3) are useful tools. Figure 3 shows mean hazard impacts and their associated 5th to 95th percentile range under present day conditions and at the end of the century under the 2.0m global SLR scenario. From these maps we see that while on average the RBLC experiences 24% collision hours by the end of the century, some areas will need to be prepared for 40 to 60% impact hours under this SLR scenario, while others will see virtually no change in erosion hazard. Furthermore, the maps contextualize where hazardous conditions occur and help us interpret their effect on the community. In RBLC, collision and beach safety hazards are focused on headlands, where erosion and sandy beach recreation may be less of a concern. However, there are also considerable collision and beach safety hazards near the mouths of estuaries, which are susceptible to erosional and beach narrowing hazards, and are of significant recreational, cultural, and economic value.

To better identify where hazard impacts will undergo the greatest change, we employ the normalized hotspot indicator metric (Figure 4). We incorporate the impact multiplier into the hotspot indicator to emphasize regions that rarely or never experience a hazard under current conditions but will experience an increase in the future. Community members in these areas may presently feel no incentive to prepare for changing conditions and may therefore be relatively unprepared for increases in hazards due to a historical sense of security.

Figure 4 highlights that the impact hours multiplier and the total difference in impact hours can have high values in different locations, but the hotspot indicator only scores highly in areas where both values are large. In RBLC, the impact multiplier for overtopping can extremely large (or infinite) as there are many locations where there is a small value of final overtopping hours divided by initial overtopping hours zero or close to zero. However, the total increase in the impact hours is also near zero, so there are very few locations that score highly on the hotspot indicator scale. Conversely, beach safety has a large increase in the total impact hours, but the impact multiplier is relatively low (as beach safety started with relatively high impact hours in the present decade). As such, the beach safety

metric also has low hotspot indicator scores. Collision is the only hazard metric that has high values for the impact multiplier and total difference in impact hours. This metric has the highest hotspot indicator scores for the RBLC region. Therefore, this community may want to focus adaptation efforts on areas with high collision hotspot scores.

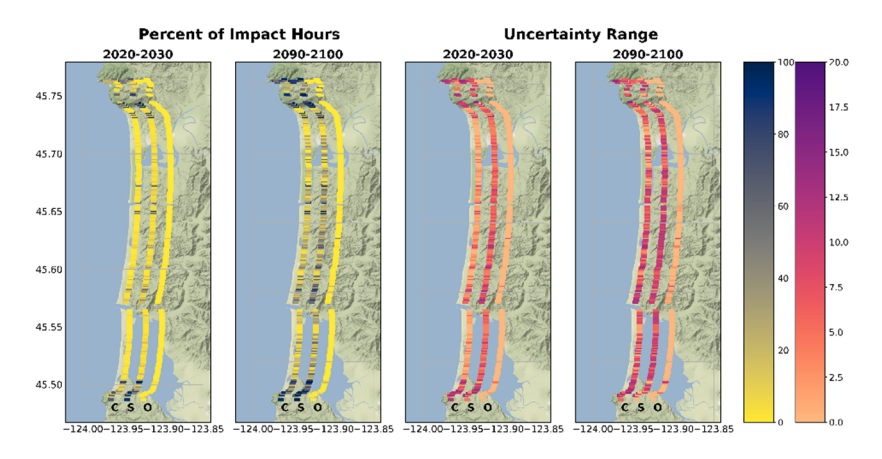


Figure 3. Percent impact hours for global SLR = 2.0m by 2100 averaged over 100 simulations during present day conditions (2020-2030) and at the end of the century (2090-2100) for collision (c), beach safety (s), and overtopping (o) hazard metrics. Panels on the right show the range of uncertainty between 95th and 5th percent confidence intervals.

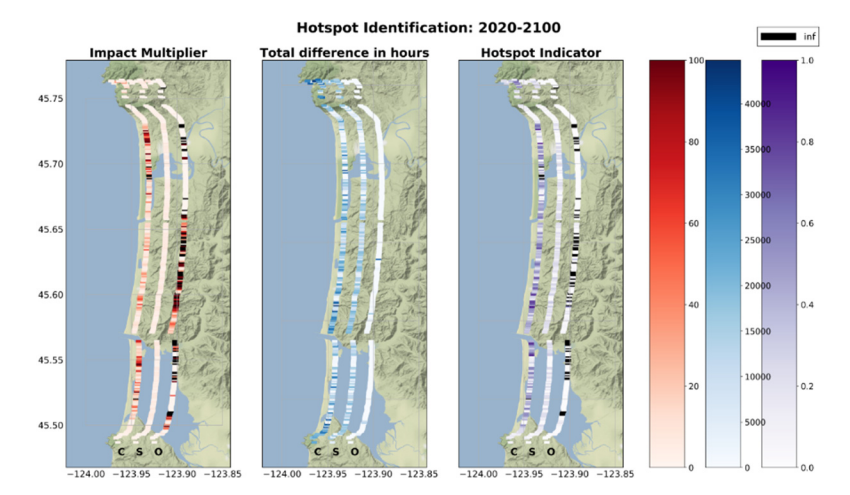


Figure 4. Metrics to identify hotspots (see Eq. 3) in future hazard activity for Rockaway Beach littoral cell under global SLR = 2.0m by 2100 for collision (c), beach safety (s), and overtopping (o) hazard metrics.

Conclusion

The results shown here for a subset of Cascadia, USA highlight how useful spatially varying, scenario-based hazard impacts assessments and hotspot indicators are for identifying which areas and types of hazards may require increased adaptation support. In the Rockaway Beach Littoral Cell (RBLC), collision and beach safety are the primary hazards impacting the coast over the next century. However probabilistic simulation modeling has shown that these hazards are highly spatially variable. Furthermore, collision hotspots are found along much of the RBLC sandy beaches, while overtopping and beach safety undergo much less dramatic changes from present day conditions even under the most extreme SLR scenario.

RBLC results also showcase the value in combining stochastic TWLs derived from TESLA with a hazard impact framework to assess uncertainty through the simulation of both chronic and extreme conditions. This approach enables us to piece apart the relative uncertainty of hazards as driven by SLR versus natural variability (caused by variation in climate, weather, and hydrodynamic drivers). Future work will focus on exploring the relative importance of ENSO (AWTs), synoptic weather (DWTs), and SLR in driving hazards in the Cascadia region over different timescales. Future work will also present a more extensive analysis of the sources of hazard impact uncertainty and how they vary spatially and temporally while expanding the presentation of results to include the full Cascadia region.

This probabilistic, regional scale hazard impact assessment was produced with deep stakeholder engagement and will be a critical component to adaptation planning efforts in the Cascadia region.

Acknowledgements

We acknowledge funding that supported this research in part from Oregon Sea Grant under Award NA18OAR170072 (CDFA 11.417) from the National Oceanic and Atmospheric Administration's National Sea Grant College Program and the Coastlines and People program of the National Science Foundation under cooperative agreement 2103713. We also thank Steve Dundas, Amila Hadziomerspahic, and the advisory council for the Oregon Coastal Futures project who together co-produced the beach safety metric explored here.

References

- Allan, J. and Komar, P. Extreme storms on the Pacific Northwest coast during the 1997–98 El Niño and 1998–99 La Niña. J. Coast. Res.18(1), 175–193 (2002).
- Allan, J., Ruggiero, P., Garcia-Medina, G., O'Brien, F., L.L, S., Roberts, J., (2015). Coastal Flood Hazard Study, vol. 47 Tillamook County, Oregon: Oregon Department of Geology and Mineral Industries special paper 274pp.
- Anderson, D., A. Rueda, L. Cagigal, J. A. A. Antolinez, F. J. Mendez and P. Ruggiero (2019). "Time-Varying Emulator for Short and Long-Term Analysis of Coastal Flood Hazard Potential." Journal of Geophysical Research: Oceans 124(12): 9209-9234. Doi:10.1029/2019jc015312
- Antolinez, J. A. A., Méndez, F. J., Camus, P., Vitousek, S., Gonzalez, E. M., Ruggiero, P., and Barnard, P. (2015). A multi-scale climate emulator for long-term morphodynamics (MUSCLE-morpho). Journal of Geophysical Research, Oceans, 121. https://doi.org/10.1002/2015JC011107
- Barnard, P. L., A. D. Short, M. D. Harley, K. D. Splinter, S. Vitousek, I. L. Turner, J. Allan, M. Banno, K. R. Bryan, A. Doria, J. E. Hansen, S. Kato, Y. Kuriyama, E. Randall-Goodwin, P. Ruggiero, I. J. Walker and D. K. Heathfield (2015). "Coastal vulnerability across the Pacific dominated by El Niño/Southern Oscillation." Nature Geoscience 8(10): 801-807. doi:10.1038/ngeo2539
- Barnard, P. L., D. Hoover, D. M. Hubbard, A. Snyder, B. C. Ludka, J. Allan, G. M. Kaminsky, P. Ruggiero, T. W. Gallien, L. Gabel, D. McCandless, H. M. Weiner, N. Cohn, D. L. Anderson and K. A. Serafin (2017). "Extreme oceanographic forcing and coastal response due to the 2015–2016 El Niño." Nature Communications 8(1): 14365. doi:10.1038/ncomms14365
- Cai, W., A. Santoso, G. Wang, S.-W. Yeh, S.-I. An, K. M. Cobb, M. Collins, E. Guilyardi, F.-F. Jin, J.-S. Kug, M. Lengaigne, M. J. McPhaden, K. Takahashi, A. Timmermann, G. Vecchi, M. Watanabe and L. Wu (2015). "ENSO and greenhouse warming." Nature Climate Change 5(9): 849-859. doi:10.1038/nclimate2743
- Cai, W., G. Wang, B. Dewitte, L. Wu, A. Santoso, K. Takahashi, Y. Yang, A. Carreric and M. J. McPhaden (2018). "Increased variability of eastern Pacific El Nino under greenhouse warming." Nature 564(7735): 201-206. doi: 10.1038/s41586-018-0776-9

- Callaghan, D., P. Nielsen, A. Short, and R. Ranasinghe (2008), Statistical simulation of wave climate and extreme beach erosion, Coastal Eng., 55(5), 375–390.
- Durrant, T., Greenslade, D., Hemar, M., and Trenham, C. (2014). A Global hindcast focused on the Central and South Pacific (technical report). CAWCR.
- Erikson, L., J. Morim, M. Hemer, I. Young, X. L. Wang, L. Mentaschi, N. Mori, A. Semedo, J. Stopa, V. Grigorieva, S. Gulev, O. Aarnes, J. R. Bidlot, Ø. Breivik, L. Bricheno, T. Shimura, M. Menendez, M. Markina, V. Sharmar, C. Trenham, J. Wolf, C. Appendini, S. Caires, N. Groll and A. Webb (2022). "Global ocean wave fields show consistent regional trends between 1980 and 2014 in a multi-product ensemble." Communications Earth & Environment 3(1): 320. doi:10.1038/s43247-022-00654-9
- Hamdi, Y., I. D. Haigh, S. Parey and T. Wahl (2021). "Preface: Advances in extreme value analysis and application to natural hazards." Nat. Hazards Earth Syst. Sci. 21(5): 1461-1465. doi:10.5194/nhess-21-1461-2021
- Haasnoot, M., Warren, A., Kwakkel, J.H. (2019). Dynamic Adaptive Policy Pathways (DAPP). In: Marchau, V., Walker, W., Bloemen, P., Popper, S. (eds) Decision Making under Deep Uncertainty. Springer, Cham. https://doi.org/10.1007/978-3-030-05252-2_4
- Hibbard, K. A. and A. C. Janetos (2013). "The regional nature of global challenges: a need and strategy for integrated regional modeling." Climatic Change 118(3-4): 565-577. doi:10.1007/s10584-012-0674-3
- Holman, R. A. (1986). "Extreme value statistics for wave run-up on a natural beach." Coastal Engineering 9(6): 527-544. doi:https://doi.org/10.1016/0378-3839(86)90002-5
- Komar, P., Allan, J. and Ruggiero, P. (2011) Sea level variations along the US Pacific Northwest coast: Tectonic and climate controls. J. of Coast. Res. 27(5), 808-823.
- Kopp, R. E., E. A. Gilmore, C. M. Little, J. Lorenzo-Trueba, V. C. Ramenzoni and W. V. Sweet (2019). "Usable Science for Managing the Risks of Sea-Level Rise." Earth's Future. doi:10.1029/2018ef001145

- Light, J. W. (2021). Morphodynamic Evolution of Coastal Oregon: Using New Lidar-derived Beach and Sand Dune Morphometrics to Explore Multidecadal Change.
- Lincke, D., J. Hinkel, M. Mengel and R. J. Nicholls (2022). "Understanding the Drivers of Coastal Flood Exposure and Risk From 1860 to 2100." Earth's Future 10(12): e2021EF002584. doi:https://doi.org/10.1029/2021EF002584
- Roelvink, D., A. Reniers, A. van Dongeren, J. van Thiel de Vries, R. McCall and J. Lescinski (2009). "Modelling storm impacts on beaches, dunes and barrier islands." Coastal Engineering 56(11): 1133-1152. doi:https://doi.org/10.1016/j.coastaleng.2009.08.006
- Sallenger, A. H. (2000), Storm impact scale for barrier islands, J. Coastal Res., 16, 890-895.
- Serafin, K. A. and P. Ruggiero (2014). "Simulating extreme total water levels using a time-dependent, extreme value approach." Journal of Geophysical Research: Oceans 119(9): 6305-6329. doi:10.1002/2014jc010093
- Serafin, K. A., P. Ruggiero and H. F. Stockdon (2017). "The relative contribution of waves, tides, and nontidal residuals to extreme total water levels on U.S. West Coast sandy beaches." Geophysical Research Letters 44(4): 1839-1847. doi:10.1002/2016gl071020
- Serafin, K. A., P. Ruggiero, P. L. Barnard and H. F. Stockdon (2019). "The influence of shelf bathymetry and beach topography on extreme total water levels: Linking large-scale changes of the wave climate to local coastal hazards." Coastal Engineering 150: 1-17. doi:https://doi.org/10.1016/j.coastaleng.2019.03.012
- Shope, J. B., L. H. Erikson, P. L. Barnard, C. D. Storlazzi, K. Serafin, K. Doran, H. Stockdon, B. Reguero, F. Mendez, S. Castanedo, A. Cid, L. Cagigal and P. Ruggiero (2022). "Characterizing storm-induced coastal change hazards along the United States West Coast." Scientific Data 9(1): 224. doi:10.1038/s41597-022-01313-6
- Shope, James B., Erikson, Li H., Barnard, Patrick L., Storlazzi, Curt D., Hardy, Matthew W., and Doran, Kara S., (2021), Modeled extreme total water levels along the U.S. west coast: data release DOI:10.5066/P95FBGZ1, U.S. Geological Survey, Pacific Coastal and Marine Science Center, Santa Cruz, California.

- Smith, G. A., Hemer, M., Greenslade, D., Trenham, C., Zieger, S., and Durrant, T. (2020). Global wave hindcast with Australian and Pacific Island Focus: From past to present. Geoscience Data Journal, 8, 1–33. https://doi.org/10.1002/gdj3.104
- Stockdon, H.F., Holman, R.A., Howd, P.A., Sallenger, A.H., 2006. Empirical parameterization of setup, swash, and runup. Coastal Engineering 53, 573–588. https://doi.org/10.1016/j.coastaleng.2005.12.005
- Sweet, W.V., B.D. Hamlington, R.E. Kopp, C.P. Weaver, P.L. Barnard, D. Bekaert, W. Brooks, M.Craghan, G. Dusek, T. Frederikse, G. Garner, A.S. Genz, J.P. Krasting, E. Larour, D. Marcy, J.J. Marra, J. Obeysekera, M. Osler, M. Pendleton, D. Roman, L. Schmied, W. Veatch, K.D. White, and C. Zuzak, 2022: Global and Regional Sea Level Rise Scenarios for the United States: Updated Mean Projections and Extreme Water Level Probabilities Along U.S. Coastlines. NOAATechnical Report NOS 01. National Oceanic and Atmospheric Administration, National OceanService, Silver Spring, MD, 111 pp.
- Taherkhani, M., S. Vitousek, P. L. Barnard, N. Frazer, T. R. Anderson and C. H. Fletcher (2020). "Sea-level rise exponentially increases coastal flood frequency." Scientific Reports 10(1): 6466. doi:10.1038/s41598-020-62188-4
- Toimil, A., I. J. Losada, R. J. Nicholls, R. A. Dalrymple and M. J. F. Stive (2020). "Addressing the challenges of climate change risks and adaptation in coastal areas: A review." Coastal Engineering 156. doi:10.1016/j.coastaleng.2019.103611
- Toimil, A., P. Camus, I. J. Losada and M. Alvarez-Cuesta (2021). "Visualising the Uncertainty Cascade in Multi-Ensemble Probabilistic Coastal Erosion Projections." Frontiers in Marine Science 8. doi:10.3389/fmars.2021.683535
- Vitousek, S., P. L. Barnard, C. H. Fletcher, N. Frazer, L. Erikson and C. D. Storlazzi (2017). "Doubling of coastal flooding frequency within decades due to sea-level rise." Scientific Reports 7(1): 1399. doi:10.1038/s41598-017-01362-7
- Yu, J. Y., X. Wang, S. Yang, H. Paek and M. Chen (2017). The Changing El Niño-Southern Oscillation and Associated Climate Extremes Climate Extremes: 1-38.